# Formation of epitaxial $Tl_2Ba_2Ca_2Cu_3O_{10}$ superconducting films by dc-magnetron sputtering and triple post-annealing method*

Xie Wei(解 伟)[a], Wang Pei(王 培)[a], Ji Lu(季 鲁)[a], Ge De-Yong(葛德永)[a], Du Jia-Nan(杜佳男)[a], Gao Xiao-Xin(高晓昕)[a], Liu Xin(刘 欣)[a], Song Feng-Bin(宋凤斌)[b], Hu Lei(胡 磊)[a], Zhang Xu(张 旭)[a], He Ming(何 明)[a], and Zhao Xin-Jie(赵新杰)[a]†

[a] *College of Electronic Information and Optical Engineering, Nankai University, Tianjin* 300071, *China*
[b] *The 10th institute of Chinese Electronic Technology Corporation, Chengdu* 610036, *China*

(Received 9 August 2013; revised manuscript received 2 January 2014; published online 22 May 2014)

For obtaining pure phase $Tl_2Ba_2Ca_2Cu_3O_{10}$ (Tl-2223) films with good superconducting properties, the growth technique is improved by dc magnetron sputtering and a triple post-annealing process. The triple post-annealing process comprises annealing twice in argon and once in oxygen at different temperatures. In the first low-temperature annealing phase in argon, $Tl_2Ba_2CaCu_2O_8$ (Tl-2212) is obtained to effectively minimize evaporation in the next step. With the increase of temperature in the second annealing stage in argon, the previously prepared Tl-2212 inter-phase is converted into Tl-2223 phase. An additional annealing in oxygen is also adopted to improve the properties of Tl-2223 films, each containing an optimal oxygen content value. The results of X-ray diffraction (XRD) $\theta$–$2\theta$ scans, $\omega$ scans and rotational $\phi$ scans show that each of the Tl-2223 films has a high phase purity and an epitaxial structure. Smooth films are observed by scanning electron microscopy (SEM). The critical temperatures $T_c$ of the films are measured to be about 120 K and the critical current densities $J_c$ can reach 4.0 MA/cm$^2$ at 77 K at self field.

**Keywords:** Tl-2223 superconducting films, post-annealing, critical temperature, critical current density

**PACS:** 74.78.–w **DOI:** 10.1088/1674-1056/23/7/077401

## 1. Introduction

In the Tl-based high temperature superconductor (HTS) family, $Tl_2Ba_2Ca_2Cu_3O_{10}$ (Tl-2223) films are attractive due to their high critical temperatures of up to 120 K.[1] The critical temperature suggests that the Tl-2223 film could be operated at higher temperature. As a result, electronic devices can be fabricated in a compact planar form, offering a significant saving in size and weight, which makes it possible to operate at temperatures over 100 K and to reduce the cost of refrigeration devices for microwave systems.[2] These potential benefits motivate us to fabricate reproducible high-quality Tl-2223 films which are more suitable for device applications. In the past several decades, many reports on the fabrication of Tl-based HTS films have been presented. Most of Tl-based films were fabricated by a two-step process involving the deposition of an amorphous precursor film (which may or may not have contained thallium), using one of the standard thin-film deposition techniques and an *ex situ* anneal in the presence of thallous oxide vapour to form the crystalline superconducting material.[3,4] The primary deposition techniques for preparing the Tl-based films are laser ablation,[5–7] spray pyrolysis,[8,9] electron beam evaporation,[10,11] organic chemical vapor deposition[12,13] and sputtering.[14–16] Some of the above-mentioned techniques for thin film fabrication need a high processing temperature, especially for annealing in oxygen. Reducing the loss of thallium during synthesis is the key to the annealing process. Many groups suggested methods to solve this problem. Firstly, Bramley *et al.*[3] pointed out that in the annealing process, the fabrication of Tl-based films involves a delicate balance between the high temperatures required to form the superconducting phases and the high volatility of thallium at these temperatures. The partial pressures of oxygen ($P(O_2)$) and thallous oxide vapour ($P(Tl_2O)$) have an effect on the optimum processing temperature. A previous investigation reported on the $O_2$ pressure–temperature stability regime for Tl-2223.[17] The maximum $O_2$ pressure could decrease as temperature decreased. This result implies that Tl-2223 films can be prepared at a temperature much lower than the 880 °C used earlier, provided that the oxygen pressure is below 1 atm.[18] Therefore, many successful preparation methods were proposed such as annealing in reduced $O_2$ pressure, in 10% $O_2$ /Ar or in the air.[18–20] Although the morphology was visibly smooth and the critical temperature $T_c$ exceeded 120 K, the critical current density $J_c$ (77 K) could not exceed 2 MA/cm$^2$ as indicated in early researches.

Secondly, knowledge of the reaction mechanisms can aid in devising new methods and conditions for preparing single-phase superconductors.[21] Kinetic studies regarding the formation of Tl-2223 in bulk were reported.[22,23] Siegal *et al.*[24] demonstrated that knowledge of both the thermodynamics and the kinetics of growth can yield high-quality films all with the

*Project supported by the National Natural Science Foundation of China (Grant Nos. 51002081 and 61176119).
†Corresponding author. E-mail: zhaoxj@nankai.edu.cn
© 2014 Chinese Physical Society and IOP Publishing Ltd 

major Tl-superconducting phase. They find that the T1-1212 or the T1-2212 phase nucleates first during film growth, no matter what the precursor film composition is. These phases can be converted into the T1-1223 or T1-2223 phases via an extended duration growth process, or by the use of higher growth temperatures. However, the best Tl-2223 films grown at 895 °C each have a zero-resistance $T_c = 115$ K and $J_c$ (5 K) $\sim 3$ MA/cm$^2$.

These results may be caused by the high temperature in the annealing process, especially if the annealing temperature is above 880 °C. At high temperature, high volatility will also lead to many pits and holes. Furthermore, the longer the annealing time, the higher the volatility in sample will be. On the other hand, before the annealing temperature rises to 880 °C–900 °C, the sample, when going through the temperature region, Tl-2212 phase is formed (830 °C–860 °C).[17] Hence, the Tl-2212 phase will be formed first in the sample. This Tl-2212 phase could be converted into a Tl-2223 phase is in the case of higher growth temperature or longer annealing time.[24] If the annealing time was not long enough, the crystal boundary will be formed by this Tl-2212 together with existent Tl-2223. Therefore, both the crystal boundary and pits could reduce the transport critical current densities.

According to the above-mentioned issues and facts, we propose the following methods. Considering the fact that the Tl-2212 film could be fabricated successfully at lower temperature (720 °C–760 °C) in pure argon,[25] we try to produce Tl-2223 film in argon at a relatively low temperature. On the basis of the crystal growth mechanism,[26] crystal nuclei are formed first in the parent material with rising temperature. On the other hand, decomposition is also existent because of the thermal motion. Owing to the atoms of parent material diffusing to the surface of crystal nuclei, the crystal nuclei could continue to grow. Only the crystal nuclei of sizes greater than the critical size could grow into crystalline grain, otherwise, the crystal nuclei will be decomposed by thermal motion. The larger the critical size of crystal nuclei, the larger the bound energy is. The critical size of crystal nuclei is also related to the growth temperature of crystalline grain. The lower the growth temperature, the smaller the critical size is. Therefore, our sample is first annealed at 720 °C–760 °C to make a Tl-2212 phase to nucleate. Smaller size crystalline nuclei can favor the diffusions of Ca and Cu into crystal nuclei of Tl-2212. On the other hand, in the annealing process, the rate of evaporation in the crystalline state is lower than that of the amorphous state. Furthermore, this sample already contained a large number of crystal nuclei of Tl-2212. Therefore, the rate of evaporation may be reduced if the sample is annealed again at high temperature. To test and verify our idea, the Tl-2223 films are fabricated on $3\times10$ mm$^2$ $LaAlO_3$ substrates. The results show that the films are smooth with good in-plane and out-of plane orientations. Moreover, the Tl-2223 films are shown to be epitaxial with a transport critical current density of 4 MA/cm$^2$ at 77 K at self field. The effect of oxygen on the superconducting properties of Tl-2223 film is also studied.

## 2. Experimental details

Tl-2223 films were prepared on (001) $LaAlO_3$ with dc magnetron sputtering and a triple post-annealing process. In dc magnetron sputtering, the Tl–Ba–Ca–Cu–O precursor films were deposited on (001) $LaAlO_3$ substrates from a pair of facing Tl-2223 superconducting targets. The targets were prepared by the solid-state reaction of stoichiometric quantities of CaO, $BaO_2$, CuO and $Tl_2O_3$ powders with an initial cation ratio of Tl:Ba:Ca:Cu=2.7:2:2:3. The substrates were positioned parallel to the symmetrical centerline of two faced targets and outside the discharge area to minimize the re-sputtering effect. Sputtering was carried out in an atmosphere of 80% argon and 20% oxygen with a pressure of about 1.5 Pa. In the sputtering process, the substrates were kept at ambient temperature. The thickness of precursor film was about 950 nm.

In the triple post annealing process, the precursor films were sealed in a special alumina crucible together with a Tl-based target that acts as a source of $Tl_2O$ vapor, and then the crucible was placed in a tube furnace. The tube was pumped out and filled with pure argon to 1 atm. In the first annealing stage, the precursor films were annealed at 720 °C–760 °C for 0.5 h–6 h. In this temperature range, the inter-phase of Tl-2212 was formed. Then, for the second annealing, the temperature of the furnace was raised to 780 °C–840 °C for 4 h–8 h to convert Tl-2212 into Tl-2223. After these two annealing processes, Tl-2223 phase was formed. For optimizing oxygen content in Tl-2223 film, a third annealing at 850 °C–880 °C for 0.5 h–8 h in oxygen was adopted.

The morphologies of Tl-2223 films were observed by scanning electron microscopy (SEM). Films were also observed by optical microscope in transmitted light mode to check whether the pits and holes in films had extended to the substrate–film interface. The structural characterizations of these films are performed by X-ray diffraction (XRD) $\theta$–$2\theta$ scans, $\omega$ scans and rotational $\phi$ scans on a Rigaku DMAX-2500 X-ray diffractometer with Cu $K\alpha$ radiation. The superconducting transition temperatures ($T_c$) were characterized by the non-contact inductance method.[27] Transport critical current densities $J_c$ were measured for Tl-2223 films using the four-point-probe technique. Before measuring $J_c$, Tl-2223 films were patterned in 20-μm-wide and 550-μm-long microbridges by photolithography and wet etching. A voltage criterion of 1 μV was used for the determination of $J_c$.

## 3. Results and discussion

### 3.1. Formation of a pure Tl-2223 phase in argon

In order to minimize the evaporation in the annealing process, Tl-2212 is first fabricated and then converted into Tl-2223 rather than annealing the precursor films directly. After the second annealing in argon, Tl-2223 films with an average thickness of 800 nm were fabricated on the $LaAlO_3$ substrates. Figures 1(a)–1(c) give XRD $\theta$–$2\theta$ patterns of films annealed at different stages, i.e., at the first annealing (Fig. 1(a)), after the second annealing (Fig. 1(b)), over-annealed in the second annealing (Fig. 1(c)) for more than 10 h. In Fig. 1(a), it is evident that the superconducting phase is Tl-2212 while the intensities of Tl-2212 peaks are not high. Furthermore, the (00$l$) peaks of the Tl-2223 phase (as marked) are observed although they are very low. With the temperature of the furnace rising to 780 °C–840 °C, the peaks of the Tl-2212 phase disappear completely and all the peaks can be indexed as (00$l$) reflections of the Tl-2223 phase and $LaAlO_3$ substrate as marked in Fig. 1(b). The rocking curve of the (00$\underline{14}$) peak of Tl-2223 for the same sample as that in the case of Fig. 1(b) is displayed in Fig. 2. The full width at half maximum (FWHM) of the (00$\underline{14}$) peak of the Tl-2223 phase is about 0.42°. These results indicate that the film possesses a good crystalline structure and orientation with the $c$-axis perpendicular to the surface of the substrate. The $\phi$ scan of the (10$\underline{13}$) peak of Tl-2223 for the same sample as that in the case of Fig. 1(b) is shown in Fig. 3. The four sharp peaks are shifted by 90° with respect to each other, which indicates that the film shows the four-fold symmetry of the Tl-2223 crystal and is oriented in the film plane. Figure 1(c) shows the XRD pattern of the film that is over-annealed in the second annealing stage. It is obvious that the main diffraction peaks can be assigned to the (00$l$) peaks of the Tl-2223 phase. Except for the Tl-2223 and substrate peaks, a peak of the Tl-1223 phase (marked by *) is present which might result from the loss of thallium in the film in the longer annealing process.

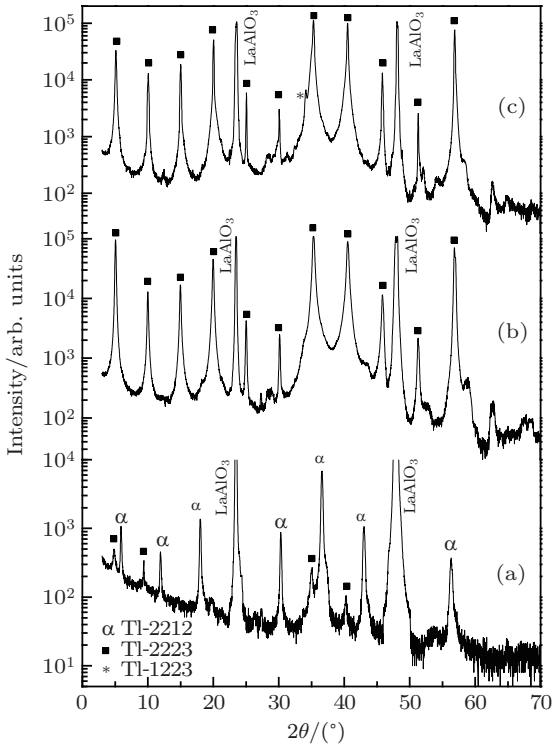



**Fig. 1.** XRD patterns of Tl–Ba–Ca–Cu–O films (a) in the first annealing stage, (b) after the second annealing stage, (c) over-annealed in the second annealing stage for more than 10 h.

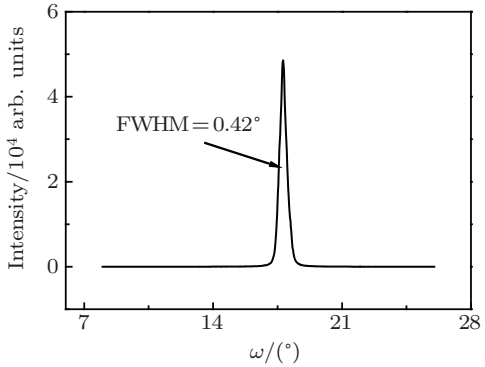



**Fig. 2.** Rocking curve of $Tl_2Ba_2Ca_2Cu_3O_{10}$ (00$\underline{14}$) after the second annealing phase.

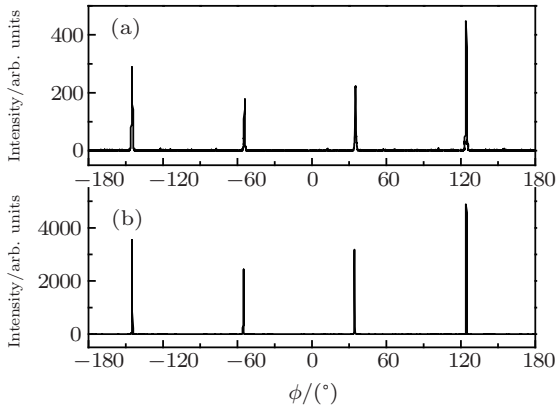



**Fig. 3.** Rotational $\phi$ scan. (a) $Tl_2Ba_2Ca_2Cu_3O_{10}$ (10$\underline{13}$) reflection and (b) $LaAlO_3$ (110) reflection.

Figures 4(a)–4(d) show the SEM images of films annealed under different conditions. Figure 4(a) shows the image of the film after the first annealing stage mentioned above. Notice that the temperature in this step is the condition of the formation of the Tl-2212 superconducting film in argon.[25] The XRD $\theta$–$2\theta$ data also indicate that there are no other reflections except the (00$l$) peaks of the Tl-2212 phase and the Tl-2223 phase as shown in Fig. 1(a). It demonstrates that the Tl-2212 and Tl-2223 crystals are formed from the precursor film, furthermore the Tl-2212 phase becomes a dominant phase in this stage. Figure 4(b) shows the surface of the film after the second annealing. In Fig. 4(b), the morphology of the film exhibits the typical features of a post-annealed HTS film, for

example, flat terraces. Figure 4(c) shows the image of the film that is over-annealed, i.e., after the second annealing for more than 10 h. In Fig. 4(c), the film shows some larger flat terraces on the surface. This result could be considered to be due to a certain extent of loss of thallium in the film during the longer annealing in the second step. If the Tl-2223 film is prepared by annealing the precursor film directly in the second annealing, the morphology of the film is somewhat poor. As given in Fig. 4(d), pits and small particles could be observed on the surface. Comparing Fig. 4(b) with Fig. 4(d), the morphology of the Tl-2223 film is improved by performing the first annealing in argon. Besides, in order to check whether holes extend to the substrate–film interface, we use the optical microscope in transmitted light mode to observe that light penetrates through the holes in the film. The result shows that only the sample of the annealed precursor film directly allows light to go through the holes. As given in Fig. 5, there are many bright dots in the film because of high temperature volatilization.

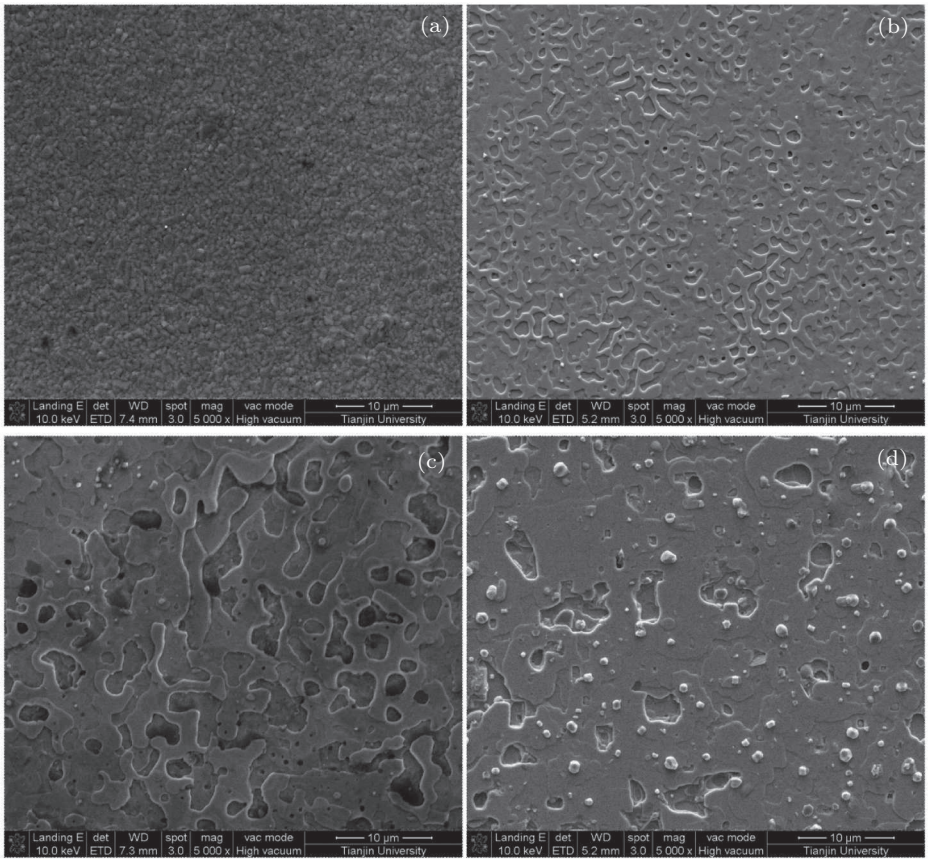



**Fig. 4.** SEM micrographs of Tl–Ba–Ca–Cu–O films annealed under different conditions respectively: (a) after the first annealing, (b) after the second annealing, (c) over-annealed in the second annealing for more than 10 h, and (d) annealing precursor film directly in the second annealing.

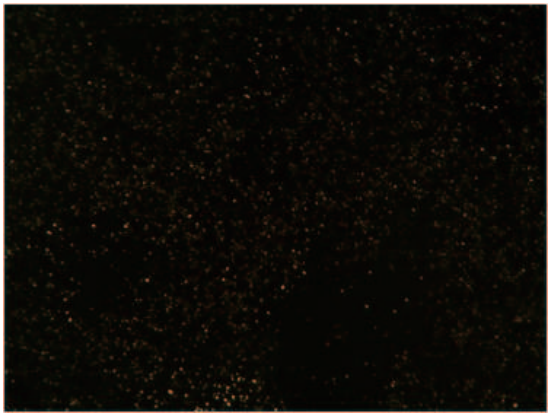


**Fig. 5.** (color online) Digital photograph of Tl-2223 film taken by a microscopic camera at 400×.

### 3.2. Optimization of the oxygen content in the Tl-2223 phase

The Tl-2212 film could be converted into a Tl-2223 film by annealing in a pure argon environment (mentioned above). The morphology of the Tl-2223 film is smooth and has no second phase. Figure 6 shows the values of the critical temperature $T_c$ of the Tl-2223 films annealed at different temperatures in the second step. With the increase of annealing temperature, the tendency of $T_c$ to rise is shown in Fig. 6. However, the highest $T_c$ of a sample annealed in argon could not exceed 116 K in our experiment as given in Fig. 6. In the self field, the critical current density $J_c$ value of the Tl-2223 film is 0.7 MA/cm$^2$ in argon, which

is a relatively low value (Fig. 7). Furthermore, the highest $J_c$ (77 K) could not exceed 1.0 MA/cm$^2$ in argon. Based on research into $YBa_2Cu_3O_{7-\delta}$ film $J_c$ improvement, the superconducting property of $YBa_2Cu_3O_{7-\delta}$ film strongly depends on the variation in the oxygen concentration.[28] The reversible oxygen content which can vary between $0 < \delta < 0.5$ is related to the transition between the non-superconducting tetragonal phase and the superconducting orthorhombic phase.[29] The variation in oxygen concentration perhaps also affects the superconducting property of Tl-2223. Furthermore, our annealing process takes place in pure argon. So now, we attempt to process Tl-2223 films by additional annealing in oxygen. After this additional annealing, the Tl-2223 films underwent several changes. The effect of $T_c$ enhancement on Tl-2223 film is more distinguishable. By performing the third annealing of Tl-2223 film in oxygen, a $T_c$ of 119 K can be obtained for annealing at 850 °C and the highest $T_c$ can reach 120 K for annealing at 880 °C as indicated in Fig. 6. The transition width is still less than 2 K. Moreover, with annealing in oxygen, the increase of the $J_c$ is more evident. In Fig. 7, at 77 K, a $J_c$ of 3.8 MA/cm$^2$ can be obtained for Tl-2223 film annealed in oxygen at 850 °C, which is about five times higher than that for Tl-2223 film after the second annealing. The highest $J_c$ (77 K) could reach about 4.0 MA/cm$^2$ for the sample annealed in oxygen at 880 °C. Through the comparison of different films, it can be illustrated that the third annealing in oxygen improves the superconducting properties. Furthermore, the purity and structure of Tl-2223 are not affected seriously by annealing in oxygen. Figure 8 shows the XRD pattern of the Tl-2223 film after the third annealing at 850 °C. It is clear that the main diffraction peaks can be assigned to the (00$l$) peaks of the Tl-2223 phase. Only small peaks (denoted by $\alpha$) at $2\theta = 37.02°$ and 43.41° corresponding to the (00$\underline{12}$) and (00$\underline{14}$) peaks of Tl-2212 phase are present. We note that this step is carried out in an oxygen atmosphere. This temperature (850 °C–880 °C) will favor the higher $Tl_2O$ partial pressure over the Tl-based target in the alumina crucible. The formation of Tl-2212 is possible by high $Tl_2O$ partial pressures during the annealing. Furthermore, the generation of the Tl-2212 phase is also due to the analogous formation condition in the temperature of the Tl-2212 phase in oxygen.[17]

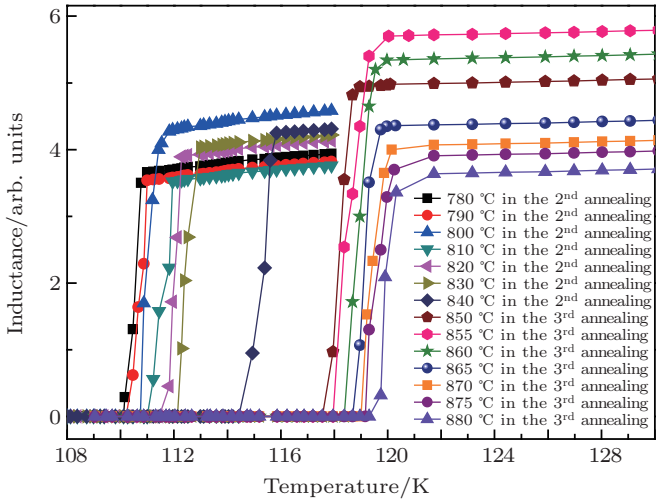



**Fig. 6.** (color online) Superconducting transition curves of Tl-2223 films after annealing in oxygen in contrast to those without the additional annealing in oxygen.

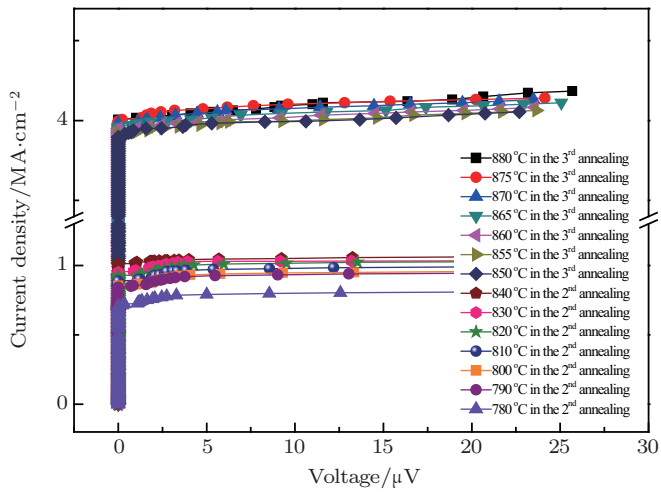



**Fig. 7.** (color online) Current density versus voltage curves of Tl-2223 films after annealing in oxygen in contrast to those without the third annealing in oxygen.

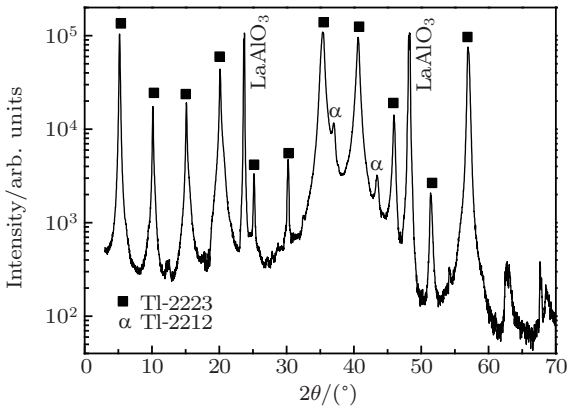



**Fig. 8.** XRD pattern of the Tl-2223 film after triple annealing.

The rocking curve of the sample is shown in Fig. 9. The FWHM of the (00$\underline{14}$) peak of the Tl-2223 phase is about 0.56°. These results could corroborate that the film possesses good crystalline structure and is entirely oriented with their $c$-axis perpendicular to the plane of the substrate surface. Figure 10 shows the image of the Tl-2223 film after the third annealing in oxygen. The film also exhibits a smooth surface morphology with a flat plate-like terrace feature which is similar to that in Fig. 4(b). The thickness of the resulting Tl-2223 film is about 800 nm.

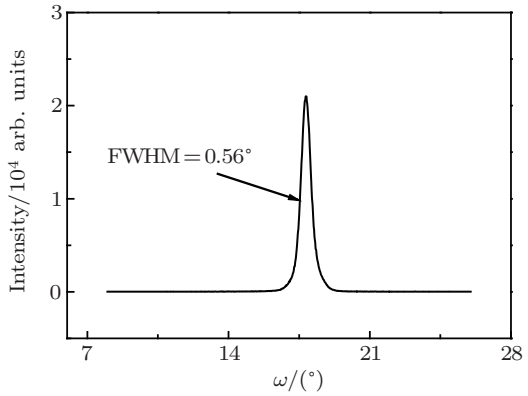



**Fig. 9.** Rocking curve of $Tl_2Ba_2Ca_2Cu_3O_{10}$ (00$\underline{14}$) after triple annealing.

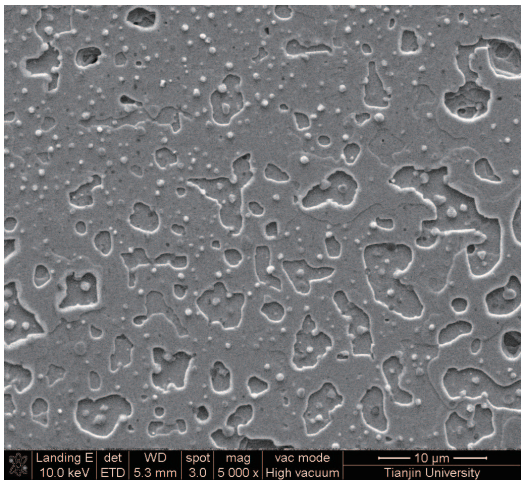



**Fig. 10.** SEM micrograph of Tl-2223 films after triple annealing.

## 4. Conclusions

In this paper, $Tl_2Ba_2Ca_2Cu_3O_{10}$ films are reproducibly prepared on (001) $LaAlO_3$ substrates by dc magnetron sputtering and a triple post-annealing method. The annealing temperature of inter-phase Tl-2212 was about 720 °C–760 °C. This is an effective reduction in temperature (compared with the 880 °C–900 °C maximum temperature which must be used in the two-step preparation process) which will minimize evaporation. The film contains a large number of crystal nuclei of Tl-2212 in this step. The rate of evaporation is reduced when the sample is annealed again at high temperature. By converting Tl-2212 into Tl-2223 in the second annealing, the Tl-2223 film is smooth and impenetrable by light in an optical microscope. The XRD measurements confirm the purity of the Tl-2223 phase in this procedure. The film exhibits flat terraces with particles. XRD $\theta$–$2\theta$ scans and rotational $\phi$ scans prove that the films are strongly textured with the $c$ axis perpendicular to the substrate's surface. The FWHM of the (00$\underline{14}$) peak of Tl-2223 on the best sample is about 0.42°. A third additional annealing in oxygen for the Tl-2223 film was also studied, which can improve the film's properties, i.e., smoother morphology and better superconducting properties. The $T_c$ of film can be obtained to be 120 K. The $J_c$ (77 K) is increased to 4.0 MA/cm$^2$ at self field. Neither the phase purity nor the crystalline structure of the film is seriously affected by the third annealing.

## References


[1] Lee W Y, Lee V Y, Salem J, Huang T C, Savoy R, Bullock D C and Parkin S S P 1988 *Appl. Phys. Lett.* **53** 329
[2] Holstein W L and Parisi L A 1996 *J. Mater. Res.* **11** 1349
[3] Bramley A P, Connor J D O and Grovenor C R M 1999 *Supercond. Sci. Technol.* **12** R57
[4] Holstein W L, Parisi L A, Wilker C and Flippen R B 1992 *Appl. Phys. Lett.* **60** 2014
[5] Liou S H, Aylesworth K D, Ianno N J, Johs B, Thompson D, Meyer D, Woollam J A and Colleen B 1989 *Appl. Phys. Lett.* **54** 760
[6] Yu Y, Shao H M, Zeng Z Y, Sun A M, Qin M J, Ren C, Xu X N, Ding S Y, Jin X, Yao X X, Zhou J, Ji Z M, Yang S Z and Zhang W L 1997 *Chin. Phys. Lett.* **14** 546
[7] Johs B, Thompson D, lanno N J, Woollam J A, Liou S H, Hermann A M, Sheng Z Z, Kiehl W, Shams Q, Fei X, Sheng L and Liu Y H 1989 *Appl. Phys. Lett.* **54** 1810
[8] Tang Y Q, Sheng Z Z, Chen Z Y, Li Y F and Pederson D O 1992 *Supercond. Sci. Technol.* **5** 538
[9] Su L Y, Grovenor C R M, Goringe M J, Jenkins A P and DewHughes D 1995 *Appl. Phys. Lett.* **66** 1542
[10] Osofsky M S, Lubitz P, Harford M Z, Singh A K, Qadri S B, Skelton E F, Elam W T, Soulen R J, Jr, Lechter W L and Wolf S A 1988 *Appl. Phys. Lett.* **53** 1663
[11] Ginley D S, Kwak J F, Hellmer R P, Baughman R J, Venturini E L, Mitchell M A and Morosin B 1988 *Physica C* **156** 592
[12] Ding F Z, Gu H W, Zhang T, Dai S T and Xiao L Y 2011 *Chin. Phys. B* **20** 027402
[13] Cassinese A, Andreone A, Gennaro E D, Pica G, Vaglio R, Malandrino G, Perdicaro L M S, Fragala I L and Granata C 2001 *Supercond. Sci. Technol.* **14** 406
[14] Huang G H, Wang X H, Xie Q L, Wang Z, You F, Ji L, Zhao X J, Fang L and Yan S L 2009 *Acta Phys. Sin.* **58** 7958 (in Chinese)
[15] Xie Q L, Yan S L, Zhao X J, Fang L, Ji L, Zhang Y T, You S T, Li J L, Zhang X, Zhou T G, Zuo T and Yue H W 2008 *Acta Phys. Sin.* **57** 519 (in Chinese)
[16] Wu C Y, Foong F, Liou S H and Ho J C 1993 *IEEE Trans. Appl. Supercond.* **3** 1205
[17] Ahn B T, Lee W Y and Beyers R 1992 *Appl. Phys. Lett.* **60** 2150
[18] Lee W Y, Garrison S M, Kawasaki M, Venturini E L, Ahn B T, Boyers R, Salem J, Savoy R and Vazquez J 1992 *Appl. Phys. Lett.* **60** 772
[19] Hinds B J, Schulz D L, Neumayer D A, Han B, Marks T J, Wang Y Y, Dravid V P, Schindler J L, Hogan T P and Kannewurf C R 1994 *Appl. Phys. Lett.* **65** 231
[20] Tang Y Q, Sheng Z Z, Lou W A, Chen Z Y, Chan Y N, Li Y F, Chan F T, Salamo G J, Pederson D O, Dhayagude T H, Ang S S and Brown W D 1993 *Supercond. Sci. Technol.* **6** 173
[21] Narain S and Ruckenstein E 1989 *Supercond. Sci. Technol.* **2** 236
[22] Ruckenstein E and Cheung C T 1989 *J. Mater. Res.* **4** 1116
[23] Cheung C T and Ruckenstein E 1990 *J. Mater. Res.* **5** 1860
[24] Siegal M P, Overmyer D L, Venturini E L, Newcomer P P, Dunn R, Dominguez F, Padilla R R and Sokolowski S S 1997 *IEEE. Trans. Appl. Supercond.* **7** 1881
[25] Yan S L, Fang L, Song Q X, Yan J, Zhu Y P, Chen J H and Zhang S B 1993 *Appl. Phys. Lett.* **63** 1845
[26] Parker R L 1970 *Solid State Phys.* **25** 151
[27] Rothwarf F, Schmitz J A, Dickson C C, Thiel R C, Boller H and Parthe E 1966 *Phys. Rev.* **152** 341
[28] Li Y J, Xiong G C, Gan Z Z, Ren C X, Chen G L and Zou S C 1993 *Acta Phys. Sin. (Overseas Edn)* **2** 211
[29] Wordenweber R 1999 *Supercond. Sci. Technol.* **12** R86